University of Massachusetts Amherst
ScholarWorks@UMass Amherst

Publications | MURI on Photomechanical Materials

2020

Donor-Acceptor Stenhouse Adducts: Exploring the Effects of Ionic Character

Miranda Sroda
University of California, Santa Barbara

Friedrich Stricker
University of California, Santa Barbara

Julie A. Peterson
University of California, Santa Barbara

Alexandria Bernal
University of California, Santa Barbara

Javier Read de Alaniz
University of California, Santa Barbara

Follow this and additional works at: https://scholarworks.umass.edu/muri_pubs

Sroda, Miranda; Stricker, Friedrich; Peterson, Julie A.; Bernal, Alexandria; and Read de Alaniz, Javier, "Donor-Acceptor Stenhouse Adducts: Exploring the Effects of Ionic Character" (2020). *Chemistry - A European Journal*. 27.
https://doi.org/10.1002/chem.202005110

This Article is brought to you for free and open access by the MURI on Photomechanical Materials at ScholarWorks@UMass Amherst. It has been accepted for inclusion in Publications by an authorized administrator of ScholarWorks@UMass Amherst. For more information, please contact scholarworks@library.umass.edu.

Check for updates

Author Manuscript

Title: Donor–acceptor Stenhouse adducts: Exploring the effects of ionic character

Authors: Javier Read de Alaniz; Miranda M. Sroda; Friedrich Stricker; Julie A. Peterson; Alexandria Bernal; Javier Read de Alaniz

This is the author manuscript accepted for publication. It has not been through the copyediting, typesetting, pagination and proofreading process, which may lead to differences between this version and the Version of Record.

To be cited as: 10.1002/chem.202005110

Link to VoR: https://doi.org/10.1002/chem.202005110

FULL PAPER

Donor–acceptor Stenhouse adducts: Exploring the effects of ionic character

Miranda M. Sroda,‡[a] Friedrich Stricker,‡[a] Julie A. Peterson,[a] Alexandria Bernal[a] and Javier Read de Alaniz*[a]

[a] M. M. Sroda, F. Stricker, J. A. Peterson, A. Bernal, Prof. J. Read de Alaniz
Department of Chemistry and Biochemistry
University of California, Santa Barbara
Santa Barbara, CA 93106 (USA)
‡ Contributed equally
E-mail: javier@chem.ucsb.edu

Supporting information for this article is given via a link at the end of the document.

Abstract: The effects of solution-state dielectric and intermolecular interactions on the degree of charge separation provides a route to understand the switching properties and concentration dependence of donor–acceptor Stenhouse adducts (DASAs). Using solvatochromic analysis of the open form DASA in conjunction with X-ray diffraction (XRD) and computational theory we analyzed the ionic character of a series of DASAs. First and third generation architectures lead to a higher zwitterionic resonance contribution of the open form and a zwitterionic closed form while second generation architecture poses less charge-separated open form and neutral closed forms. This can be correlated to equilibrium control and photoswitching solvent compatibility. Due to the high contribution of the zwitterionic resonance form of a first and third generation DASA we demonstrate external control over their switching kinetics by ion concentration, while second generation DASAs are less affected. Importantly, these results show how the previously reported concentration dependence of DASAs are not universal and DASAs bearing a more hybrid structure in the open form can achieve photoswitching at high concentrations.

Introduction

Donor–acceptor Stenhouse adducts (DASAs) are a particularly interesting new class of photoswitches due to their negative photochromism, visible light activation, polarity and molecular volume change.[1–4] Upon irradiation DASAs are converted from a highly light-absorbing colored form to a colorless and transparent form with overall switching kinetics highly dependent on the DASA architecture and surrounding environment. Because the closed form of DASA are not light responsive and the recovery to the open form is thermally driven, the obtained steady state upon irradiation is better described as a photothermalstationary (PTS) state rather than as a photostationary state.[5] Since their discovery in 2014, these molecules have been exploited in a number of applications including targeted drug release,[2,6,7] orthogonal photoswitching,[8] chemical and thermal sensing,[9–12] and most recently fluid velocity control and photothermal actuation.[13] Synthetic efforts have resulted in three generations of DASAs which vary in photoswitching properties such as thermodynamic equilibrium between the open and closed form in the absence of light irradiation, wavelength tuneability (500–700 nm), switching rates, and solvent dependence.[1–4] The first generation, published in 2014, consisted of strongly electron donating dialkylamine donors and Meldrum's or Barbituric acid acceptors (Figure 1).[1,2] These derivatives show excellent equilibrium control and fatigue resistance, but are limited in wavelength tuneability and solvent compatibility – defined herein as the ability to switch reversibly upon irradiation in a range of solvents. In 2016 the second generation of DASAs was introduced by employing weakly donating cyclic and acyclic aryl amines (Figure 1).[3,14] These show improved wavelength tuneability (500–700 nm), and enhanced switching properties including low PTS, higher solvent compatibility and solid-state switching, but show compromised thermodynamic equilibrium in the dark (~50–7% open form in the absence of light) and extended half-lives of the closed form. The third generation in 2018 introduces strongly electron withdrawing carbon acids (Figure 1). These derivatives have enhanced switching properties such as increased solvent compatibility and tunable half-lives of the closed form, while maintaining high equilibrium control.[4] The synthetic effort has been tightly coupled with extensive mechanistic studies by Feringa, Beves, Martinez, Marazzi and others.[14–20] Here it has been demonstrated that the actinic *Z-E* isomerization step is independent of solvent and concentration and occurs on a fs-ns timescale.[17,21] This is followed by a C_3-C_4 bond rotation and thermal 4π–electrocyclization leading to the ring-closed cyclopentenone with a *trans* relationship between the C_1 and C_5 groups, that occurs on a ns-ms timescale (Figure S3). In contrast to the actinic step, the thermal part of the mechanism is highly solvent and concentration dependent.[17,21] Further use of DASA in more widespread applications has been hampered by limited understanding of solvent compatibility and most importantly concentration dependence. The concentration dependence first reported by Bardeen and our group in 2019 shows decreasing half-lives of the closed isomers at increased concentration while also lowering overall quantum yields.[21] This severely hinders applications requiring high concentration of DASA molecules. To further enable the use of DASA photoswitches it is critical that we understand and overcome the factors governing DASAs solvent compatibility and concentration dependency.

Herein we investigate medium effects on the charge-separation of DASAs through a series of XRD analysis, solution-state studies and time dependent pump probe UV-Vis spectroscopy. This work builds on three important independent preliminary studies by Beves,[14,20] Jacquemin[22] and Feringa[23] that show the zwitterionic character of the open form of DASAs.

This article is protected by copyright. All rights reserved

Author Manuscript

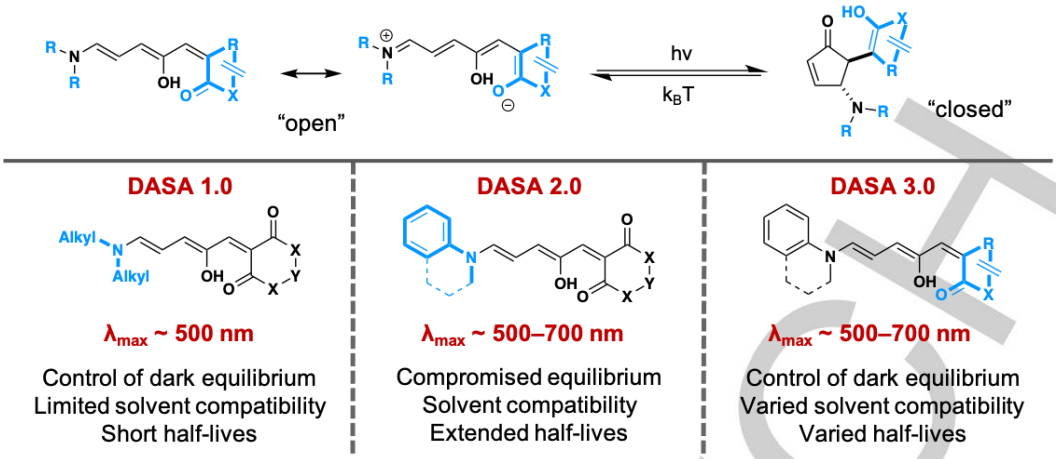

Figure 1. Synthetic efforts have resulted in three generations of DASAs which vary in photoswitching properties including control of thermodynamic equilibrium, solvent compatibility and switching kinetics. The closed form is only depicted with the acceptor group in the enol form, however, as reported in the literature the closed form can reside in either a zwitterionic, enol, or keto form depending on the architecture and conditions.[1,3,14]

Using XRD data, Beves and co-workers have reported open linear zwitterionic forms for first and second generation DASAs, concluding the polyene system in second generation DASAs are significantly delocalized.[14,20] In a separate theoretical investigation, Jacquemin reported that the Mulliken charge for first generation DASAs in both the open and closed form have a significantly negative charge (-0.54 e and -0.56 e, respectively), suggesting both have a zwitterionic nature.[22] Furthermore, they calculated the open and closed DASA isomers which have similar and large ground-state dipole moments that exceed 15D. Feringa used solvatochromic analysis to investigate the role of the hydroxyl group on the photoisomerization pathway.[23] In addition, Wagner recently reported the effect of this zwitterionic character on DASA fluorescence emission and its effects on first generation DASA in protic solvents.[24] Despite these initial reports, no effort has been made to understand the implications of the ionic character of the open form of DASA on solvent compatibility and concentration effects. By using solvatochromic shift analyses, XRD and charged ionic liquids as a dopant, we demonstrate how the ionic character of DASA influences their solvent compatibility and concentration effects.

Results and Discussion

For this study, we selected DASA derivatives which range in photoswitching properties including thermodynamic equilibrium between the open and closed form in the absence of light irradiation, solvent compatibility, photothermalstationary state, and half-life (Figure 3A, properties summarized in Table S1). As a first generation DASA we choose **DASA 1-MM** consisting of a dimethylamine donor and a Meldrum's acid derived acceptor. This derivative has high thermodynamic equilibrium control in chloroform with 94% in the open form in the dark (for experimental detail see the supporting information in section 6). This compound also exhibits a short half-life in chloroform (172 s) leading to a PTS of 76%. For a second generation derivative we choose **DASA 2-IM** bearing an indoline-based donor with a Meldrum's acid acceptor. Compared to **DASA 1-MM**, it suffers from a compromised thermodynamic equilibrium with only 50% residing in the open form in the dark and an extended half-life of the closed form of 3,240 s in chloroform. However it also shows reversible switching in more polar solvents such as acetonitrile.[4] To represent a third generation DASA derivative we selected **DASA 3-IP** bearing an indoline-based donor and CF_3 pyrazalone-based acceptor. This derivative has excellent thermodynamic equilibrium control with >95% in the open form in the dark and a short-lived closed form with a half-life of 5 s in chloroform. In contrast to **DASA 2-IM** and many second generation DASAs, this compound does not exhibit switching in acetonitrile.[4] The first and third generation derivatives show very similar behavior with high thermodynamic equilibria and short half-lives while being limited to apolar solvents like chloroform. To round out this study, DASA derivative **DASA 4-II** was chosen, which shows linear photodegradation upon irradiation and no recovery (Figure S6 compares **DASA 3-IP** and **DASA 4-II-H** photoswitching).[4]

Solid-state analysis of the ionic character of DASAs: X-ray structural analysis of the open form provides valuable insight into the ground state ionic character in the solid state.[3,20] Bond length alternation (BLA) patterns were used to analyze the ionic character, where a negative BLA value indicates zwitterionic character.[14,20] To compare the crystal structures of DASA derivatives we grew single crystals of **DASA 2-IM-H, 3-IP-H**, and **4-II-H** and used previously reported XRD data.[1,14,20] Single crystals of **DASA 2-IM-H, 3-IP-H**, and **4-II-H** were obtained using layer diffusion and slow evaporation crystallization techniques detailed in the supporting information section 4. Previously reported **DASA 1-EM**[1] was utilized due to increased crystallinity provided by the diethylamine donor in contrast to **DASA 1-MM**. In addition, DASA derivatives bearing non-methylated indoline donors (**DASA 2-IM-H** and **DASA 3-IP-H** indicated by "-H" in the label), were used as model compounds for **DASA 2-IM** and **DASA 3-IP**, respectively. As expected, for **DASA 1-EM**, bearing a strongly donating alkyl donor, the bond length alternation ($BLA_{DASA\ 1\text{-}EM}$ = -0.056 Å) show a more zwitterionic form compared to the weakly donating indoline-based donors for **DASA 2-IM-H** and **DASA 3-IP-H** which have similar, hybrid-zwitterionic ground states ($BLA_{DASA\ 2\text{-}IM}$ = -0.013 Å and $BLA_{DASA\ 3\text{-}IP}$ = -0.018 Å).

Author Manuscript

This article is protected by copyright. All rights reserved

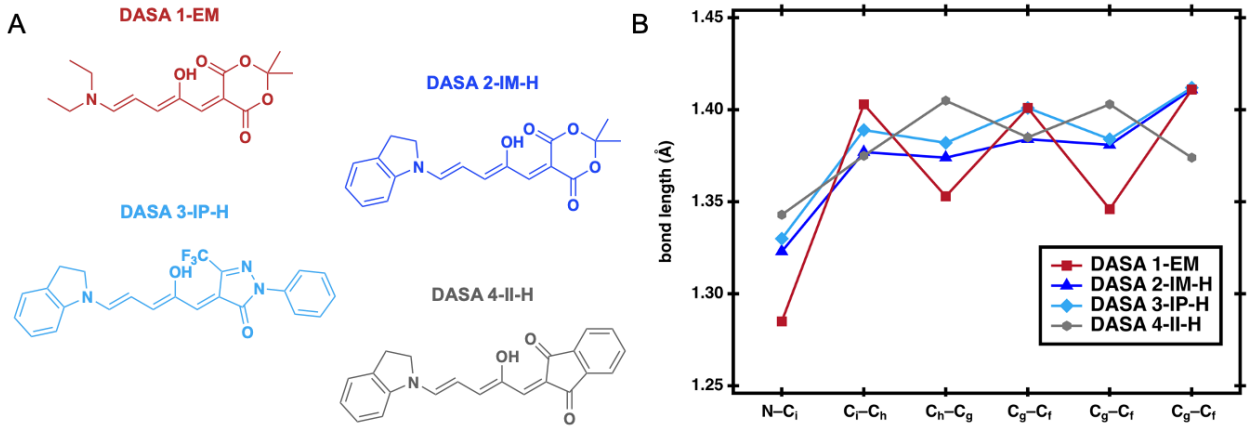

Figure 2. A. Photoswitches that were used for XRD study. **B**. Bond length alternation (BLA) patterns along the triene of the open form of DASA from XRD single crystals. For BLA calculations only the C–C bonds are taken into account. DASAs with diethylamine and non-methylated indoline donors were used as model compounds due to increased crystallinity compared to their counterparts with dimethylamine and 2-methylindoline donors.

Herein, we define hybrid as having a more delocalized conjugated triene system. Interestingly, **DASA 4-II-H**, with irreversible photoswitching, reveals opposite alternating bond slopes ($BLA_{\textbf{DASA 4-II-H}}$ = 0.026 Å) and resides in a more neutral ground state, as shown in Figure 2B. This is in agreement with previous XRD reported results that nonphotochromic spirooxazines predominantly reside in a neutral "quinoidal" structure.[25] To further extend this study, we compared the BLA of thirteen previously published open form crystals,[1,14,20] in addition to the three crystals grown in this study, shown in Figure S14 and Table S2. In most cases, the XRD data supports that photoswitching DASA molecules evaluated using this approach have some zwitterionic character in the solid state as exemplified by negative bond length alternation values ranging from -0.013 to -0.056 Å (Table S2). Inversely, **DASA 4-II-H**, has the most positive BLA of 0.026 Å and shows linear photodegradation and irreversible switching. These results suggest that a charge-separated, hybrid/zwitterionic ground state is an important design principal for photoswitchable DASAs. Of note, the BLA from the crystal structures revealed similar results for both the second and third generation derivatives (-0.013 Å and -0.018 Å) which is not consistent with the vastly different photoswitching behavior in solution between the two generations. This is not surprising since XRD relies on single crystalline environment while DASA's photoswitching properties have been shown to be highly dependent on environmental factors like solvent and concentration.

Solution-state analysis of the ionic character of DASAs: To gain insight into the charge-separation of DASAs in solution, we analyzed solvatochromic shifts of DASA derivatives. For this we utilized the Dimroth–Reichardt E_T solvent polarity scale to explore the dipolar nature of DASA.[25] The Dimroth–Reichardt E_T^N solvent polarity scale takes into account solvation effects arising from both nonspecific (e.g., dipole-dipole, induced dipole-induced dipole) and specific (e.g., hydrogen bonding) interactions, where the slope can provide insight into the difference in dipolar character between the ground state and the excited state. A negative solvatochromic slope (blue-shifts in more polar solvents), suggests a stabilization of the zwitterionic ground state with increasing solvent polarity. Inversely, a positive solvatochromic slope suggest a more dipolar excited state which is stabilized with increasing solvent polarity. The scale is based on the electronic transitions of a polarity probe dye in a range of solvents which is normalized to nonpolar tetramethylsilane (TMS) (E_T^N = 0) and polar water (E_T^N = 1.0). The features of the absorption bands were correlated with the Dimroth-Reichardt E_T^N solvent polarity scale of ten solvents (Table S3).[26] Photoswitches studied and their corresponding photoswitching properties (thermodynamic equilibrium, PTS, and thermal half-life) in chloroform are shown in Figure 3A. Figure 3B shows the blue–shift of the absorption band of **DASA 3-IP** with increasing solvent polarity. Figure 3C shows absorption maximum vs the polarity value of the solvents of the four DASA derivatives. **DASA 1-MM**, **DASA 2-IM**, and **DASA 3-IP** all show negative solvatochromic shifts (blue-shifts in more polar solvents), suggesting a stabilization of the zwitterionic ground state with increasing solvent polarity (with a slope ranging from -7 to -60 nm shown in Table 1 and Figure S20). Interestingly, **DASA 4-II-H** shows a positive solvatochromic shift with a slope of 14 nm (red-shift in more polar solvents), suggesting a more dipolar excited state which is stabilized with increasing solvent polarity. In agreement with the XRD results, this suggests that the dipolar nature of reversible and non-reversible DASAs are different.

To gain a better understanding of the varying contribution of the zwitterionic resonance form we compared the negative slopes of the reversible switching DASAs. The slopes of **DASA 1-MM** and **DASA 3-IP** are comparable with slopes at -46 and -60 nm. This is in contrast to the XRD data where **DASA 3-IP** seems to have less zwitterionic character than **DASA 1-MM**. **DASA 2-IM**, however, has a significantly lower negative shift, with a slope of -7 nm supporting a hybrid character shown by XRD. The more pronounced negative solvatochromism of **DASA 1-MM** and **DASA 3-IP** suggests that these derivatives have more zwitterionic character than **DASA 2-IM**. These results correlate with the respective electronic character of the donor and acceptor. **DASA 1-MM** has a strongly donating alkylamine donor and a weakly withdrawing Meldrum's acid-based acceptor while **DASA 3-IP** consists of a weaker arylamine donor and a strongly electron withdrawing CF_3-Pyrazolone-based acceptor. **DASA 2-IM** consists of both a weak donor and acceptor, resulting in overall weaker charge separation or hybrid structure. The highly charge-separated DASAs (**DASA 1-MM** and **DASA 3-IP**) show similar behavior in switching properties including a high percent

This article is protected by copyright. All rights reserved

Author Manuscript

of open form in the dark (94 and >95% in chloroform), fast thermal reversion ($t_{1/2}$ = 173 s and 5 s), and limited solvent capability. In contrast, **DASA 2-IM** is less sensitive to the environment and experimentally switches in a wider range of solvents but has a compromised equilibrium. Beves reported absorption profiles for a series of second generation DASAs bearing aniline-based donors in various solvents. In agreement with our observed trend, these solvatochromic slopes can be correlated with the relative dark equilibrium (Figure S21).[14] The solvatochromic shifts reveal the dipolar nature of DASA and provides a simple experimental method to help understand switching properties of different DASA derivatives while also providing a more accurate representation of the push-pull system compared to XRD. Feringa[27] and Marazzi[19] have both independently shown in theoretical studies that the increasing zwitterionic resonance contribution lowers the energy barrier of the thermal reversion between A and A' (Figure S3) which is consistent with our results. This inhibits switching in more polar solvents, as thermal reversion outcompetes electrocyclization. To extend this study to polymers, we analyzed absorbance shifts within polymer blends which have been shown to facilitate photoswitching.[12,28–30] The same trend in negative slopes were observed in the polymer blends supporting that DASA photoswitching molecules also have a high degree of charge-separation in the ground state in solid macromolecular environments (Figure S22).

With a better understanding of the contribution of the zwitterionic resonance open form, we were also interested in evaluating the ionic character of the closed form (supporting information section 13). Previous reports have shown the closed form of first generation DASAs with alkyl donors to be zwitterionic while second generation have been shown to form neutral (keto or enol) closed form isomers via 2D-NMR analysis.[14,20] There have been no reports on closed form isomers for third generation derivatives. In accordance with literature reports, 2D-NMR analysis shows a zwitterionic closed form for **DASA 1-MM** (Figure S25–S26) and a neutral (keto) closed form for **DASA 2-IM** (Figure S30–S31). Interestingly, despite the weakly donating indoline-based donor, 2D-NMR analysis reveals a zwitterionic closed form for **DASA 3-IP** similar to first generation DASAs (Figure S34–S35).

Computational calculations: Our results from the solvatochromic analysis are supported by theoretical calculations using M06-2X/6-31+G(d,p) in toluene, chloroform, and acetonitrile with the SMD solvent model using Gaussian16 software.[31–34] The calculated dipole moments and BLAs in chloroform were compared with the experimental results summarized in Table 1 and supporting information section 14. Importantly, the calculations trend with the solvatochromic slopes (extracted from Figure 3B from linear trends). Where **DASA 1-MM**

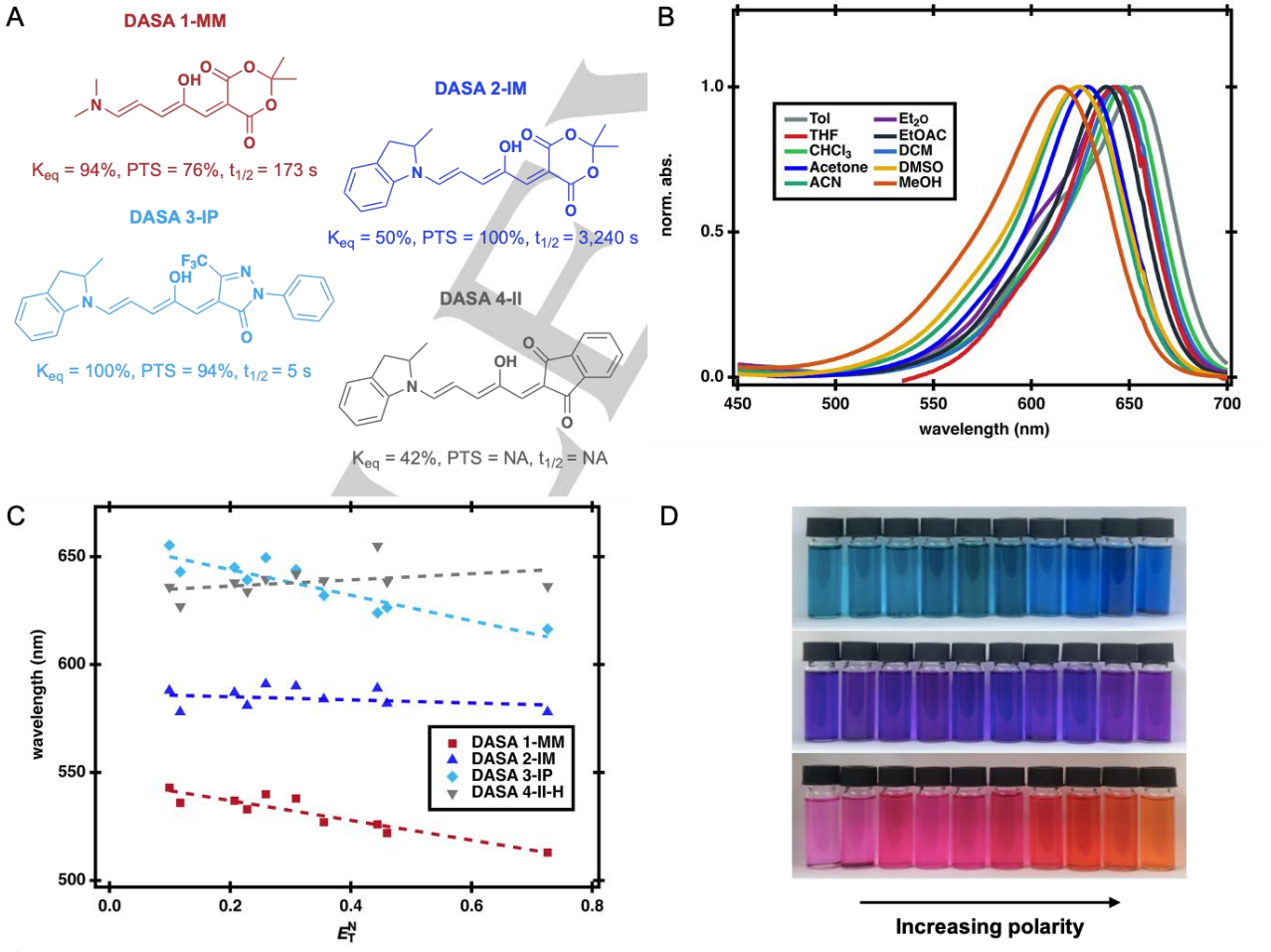

Figure 3. A. DASA derivatives studied with thermodynamic equilibrium, photothermal stationary state, and thermal half-life in chloroform for each DASA. **B**. UV–Vis traces of **DASA 3-IP** in a range of solvents, which shows a blue-shift with increasing polarity of the solvent. **C**. Solvatochromic shift analysis for **DASA 1-MM, 2-MI, 3-IP** and **4-II-H** in solvents of different polarity using the Dimroth–Reichardt E_T solvent polarity scale. **D**. Solvatochromic trends of **DASA 3-IP** (top), **DASA 2-IM** (middle) and **DASA 1-MM** (bottom) are visible by eye, where **DASA 3-IP** and **DASA 1-MM** are more sensitive to the environment than **DASA 2-IM**.

Author Manuscript

This article is protected by copyright. All rights reserved

Table 1. Experimental data compared to computational calculations.

DASA	Slope[a]	BLA[b]	Dipole[c]	BLA[c]
DASA 3-IP	-60	-0.018	17.4	-0.010
DASA 1-MM	-46	-0.056	14.7	-0.007
DASA 2-IM	-7	-0.013	12.0	0.010
DASA 4-II	14	0.026	9.0	0.023

[a] Solvatochromic slopes (nm) extracted by a linear trend from Figure 3B. [b] Bond length alternation (Å) values are extracted from XRD data of the model compounds **DASA 1-EM, DASA 2-IM-H**, **DASA 3-IP-H** and **DASA 4-II-H** shown in Figure 2. [c] Dipole (D) and BLA (Å) calculated using M06-2X/6-31+G(d,p) in chloroform using the SMD solvent model.

and **DASA 3-IP** have the highest calculated dipole and most negative BLA values, in agreement with the more negative solvatochromic slopes. Consistent with experimental results, **DASA 4-II** has the smallest dipole and the most positive BLA. Interestingly, the solvent polarity vs the HOMO-LUMO energy levels show the HOMO-LUMO gap in **DASA 2-IM** is relatively unchanged as a function of solvent, while the gap of **DASA 3-IP** increases with increasing solvent polarity in agreement with the blue-shift observed in the solvatochromic study (Figure S42). The calculations also revealed the change in the hydrogen bond length between the –OH and the carbonyl of the acceptor as a function of solvent (Figure S43). The hydrogen bond in **DASA 3-IP** is strengthened in more polar solvents compared to **DASA 2-IM**. It is possible this hydrogen bond plays a key role in stabilizing the open form in the absence of light, resulting in equilibrium control.

Influence of ionic character of DASA on photoswitching: To study the importance of the ionic character of DASA derivatives on their switching kinetics, we next sought to demonstrate the ability to tune switching kinetics by using ion concentration as an external trigger. For this, we utilized 1-butyl-3-methylimidazolium hexafluorophosphate (**IL** for ionic liquid, structure in Figure S2) as an ion pair soluble in organic solvents. We added 1 mM and 10 mM **IL** to each derivative and monitored the rate of the forward photoswitching and thermal back reaction (k_B) using time dependent pump probe UV-Vis spectroscopy. For experimental detail see the supporting information in section 15. For **DASA 1-MM** upon addition of **IL** we see a significant decrease in the forward reaction rate under light irradiation with 10 mM **IL** almost completing inhibiting photoswitching (Figure 4A). Due to low solubility of the closed form at higher concentration we were unable to obtain a thermodynamic equilibrium and therefore switching kinetics. For **DASA 2-IM**, bearing the most neutral open and closed form, a slight decrease in the forward reaction kinetics is observed with only a small effect on the recovery to the open form (k_B increases from 0.006 to 0.008 min^{-1} upon the addition of 10 mM of **IL**; rate increase of 1.4-fold) (Figure 4B). Although less dramatic than **DASA 1-MM**, the addition of **IL** to a solution of **DASA 3-IP** also resulted in a change in PTS from 89% to 55% under light irradiation. After irradiation of **DASA 3-IP** is stopped we can observe a 2.3-fold increase in the recovery rate from 7.9 min^{-1} to 17.8 min^{-1} upon the addition of 10 mM of **IL**. Taken together, these results highlight that the change in PTS results out of a combination of a decrease in forward reaction rate and an increased recovery (Figure 4C).

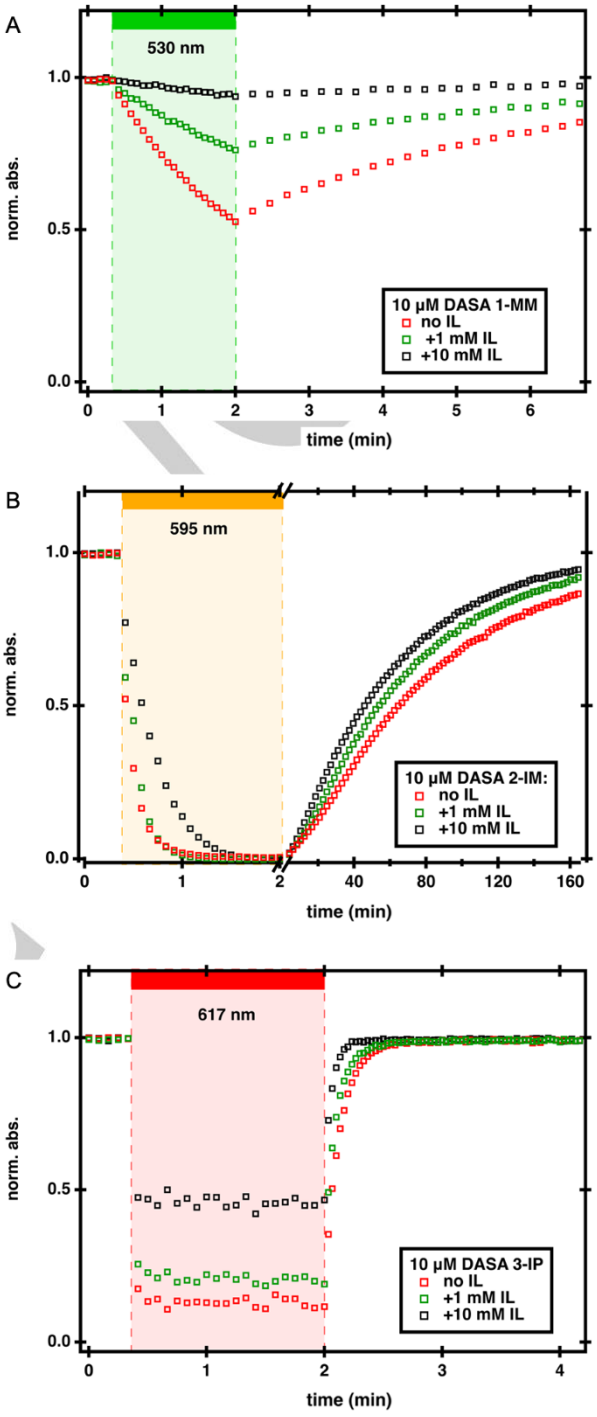

Figure 4. Influence of ionic character of DASA derivatives on its switching kinetics using an ion concentration as an external trigger. Photoswitching kinetics measured using time dependent pump probe UV-Vis spectroscopy measured at 10 µM in chloroform at their respective λ_{max} including a control without **IL** and the addition of 1 mM or 10 mM **IL**. Irradiation was started at t = 0.3 min and ceased at t = 2.0 min and the subsequent thermal recovery in the dark was measured. **A**. Time dependent UV-Vis of **DASA 1-MM** monitored at 540 nm, λ_{max}, irradiated with a 530 nm LED. **B**. Time dependent UV-Vis of **DASA 2-IM** monitored at 591 nm, λ_{max}, irradiated with a 595 nm LED. **C**. Time dependent UV-Vis of **DASA 3-IP** monitored at 647 nm, λ_{max}, irradiated with a 617 nm LED.

Author Manuscript

This article is protected by copyright. All rights reserved

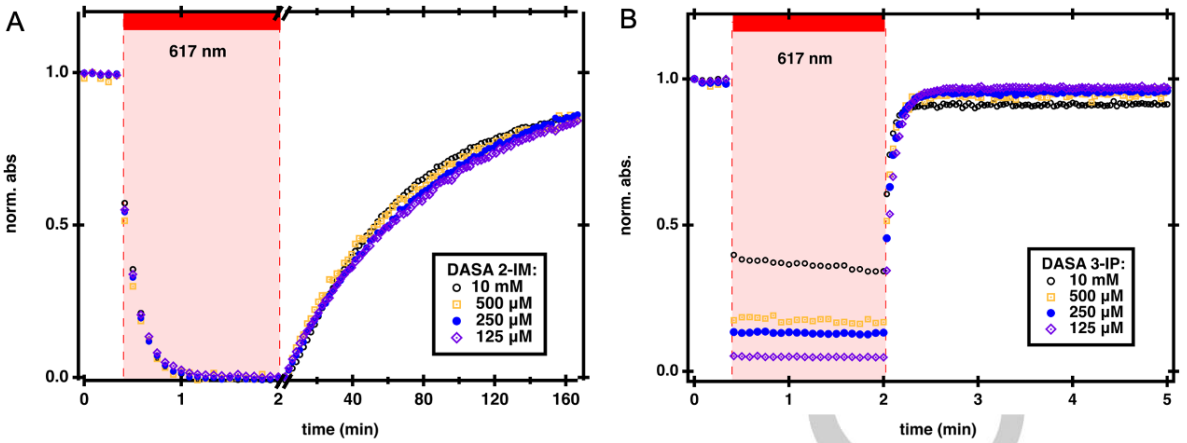

Figure 5. Influence of increasing concentration of DASA derivatives on its switching kinetics using time dependent pump probe UV-Vis spectroscopy equipped with a flow cell with variable pathlengths. Concentrations were measured from 125 µM to 10 mM and the samples irradiated with a 617 nm LED. Irradiation was started at t = 0.3 min and ceased at t = 2.0 min and the subsequent thermal recovery in the dark was measured. **A**. Time dependent UV-Vis of **DASA 2-IM** monitored at 591 nm, λ_{max}. **B**. Time dependent UV-Vis of **DASA 3-IP** monitored at 647 nm, λ_{max}.

Influence of ionic character mimics observed concentration effects: The switching properties of DASA derivatives with highly charge-separated open and closed forms, such as **DASA 1-MM** and **DASA 3-IP**, can be tuned by modifying the ionic character of the solution. In contrast **IL** addition to DASA derivatives with hybrid open and neutral closed forms, such as **DASA 2-IM**, has only a small effect on switching kinetics. These results mirror the previously reported concentration dependence of **DASA 3-IP** suggesting that the higher contribution of the zwitterionic resonance form of **DASA 3-IP** might be responsible for reduced photoswitching observed at high concentrations. To test this hypothesis, we compared the effect of concentration on the less charge-separated **DASA 2-IM** and the more charge-separated **DASA 3-IP** using time dependent pump probe UV-Vis spectroscopy equipped with a liquid cell with variable pathlengths. For experimental detail see the supporting information in section 1.2.7. The hybrid **DASA 2-IM** shows a negligible change in PTS at concentrations from 125 µM to 10 mM (Figure 5A), with a recovery rate increasing from 0.0058 min^{-1} at 125 µM to 0.0067 min^{-1} at 10 mM. In contrast, the concentration effect on **DASA 3-IP** is more dramatic. Here, we see a change in PTS from 91% to 64% and a 1.6-fold increase in recovery (10 min^{-1} at 125 µM to 16 min^{-1} at 10 mM) as the concentration increases (Figure 5B), which is consistent with previously reported results.[21] Similar experiments with **DASA 1-MM** were unsuccessful due to limited solubility of the closed isomer at concentration above 100 µM. These results reveal that the previously reported concentration dependence is not universal to all DASA derivatives, such as **DASA 2-IM** which has a PTS of 100% at 10 mM. Importantly, these results provide a path towards designing DASA derivatives able to operate at high concentrations by lowering the ground-state charge-separation in the open form and enabling the formation of a neutral closed isomer.

Conclusion

The effects of solution-state dielectric and intermolecular interactions on the degree of charge separation provides a route to understand the switching properties and concentration dependence of donor–acceptor Stenhouse adducts (DASAs) in solution. Using easy to perform solvatochromic analysis, the absorption can be used to correlate switching behavior and charge-separation in conjunction with X-ray diffraction (XRD), computational theory, and time dependent pump probe UV–Vis spectroscopy. We show that DASAs bearing the first and third generation architectures have higher contributions of the zwitterionic resonance form and zwitterionic closed forms in solution while the second generation exhibits a hybrid open form and neutral closed isomer. Furthermore, the **DASA 4-II-H** exhibits a different dipolar nature and could be a potential reason for its irreversible switching behavior. Importantly, we highlight the influence of ionic character of DASAs on their photoswitching properties through the addition of ionic liquids. The more hybrid **DASA 2-IM** shows only limited change in switching behavior upon addition of the ionic liquid, whereas **DASA 1-MM** and **DASA 3-IP** bearing a more zwitterionic open and closed form show a more dramatic effect. Additionally, we show that the previously reported concentration dependence of **DASA 3-IP** relies on the ionic character of the respective open and closed form with more hybrid **DASA 2-IM** being less affected. These results highlight the importance of the charge-separation of DASA on their switching kinetics and the ability to influence certain DASA derivatives through external stimuli. To achieve photoswitching of DASAs at high concentration a more hybrid DASA architecture should be used. Furthermore, these results enable the design of less concentration dependent DASA overcoming a major challenge for applications needing high concentrations of DASA photoswitches as organic photomechanical materials.

Acknowledgements

This work was primarily supported by the Office of Naval Research through the MURI on Photomechanical Material Systems through Grant No. ONR N00014-18-1-2624. Views and conclusions are those of the authors and should not be interpreted as representing official policies, either expressed or implied, of the U.S. Government. Use was made of computational facilities

Author Manuscript

This article is protected by copyright. All rights reserved

purchased with funds from the National Science Foundation (CNS-1725797) and administered by the Center for Scientific Computing (CSC). The CSC is supported by the California NanySystems Institute and the Materials Research Science and Engineering Center (MRSEC; NSF DMR 1720256) at UC Santa Barbara. MS wants to thank UCSB for a Graduate Opportunity Fellowship. FS wants to thank the German National Merit foundation for an ERP-scholarship. J.A.P acknowledges the support of the Elings Prize Fellowship from the California NanoSystem Institute at University of California, Santa Barbara. We also thank Dr. Guang Wu (UCSB) for X-ray analysis.

Keywords: Donor–acceptor Stenhouse adducts • photoswitch • charge-separation • solvatochromism • concentration-dependence • tunable kinetics

[1] S. Helmy, S. Oh, F. A. Leibfarth, C. J. Hawker, J. Read de Alaniz, *J. Org. Chem.* **2014**, *79*, 11316–11329.

[2] S. Helmy, F. A. Leibfarth, S. Oh, J. E. Poelma, C. J. Hawker, J. Read de Alaniz, *J. Am. Chem. Soc.* **2014**, *136*, 8169–8172.

[3] J. R. Hemmer, S. O. Poelma, N. Treat, Z. A. Page, N. D. Dolinski, Y. J. Diaz, W. Tomlinson, K. D. Clark, J. P. Hooper, C. Hawker, et al., *J. Am. Chem. Soc.* **2016**, *138*, 13960–13966.

[4] J. R. Hemmer, Z. A. Page, K. D. Clark, F. Stricker, N. D. Dolinski, C. J. Hawker, J. Read de Alaniz, *J. Am. Chem. Soc.* **2018**, *140*, 10425–10429.

[5] K. Stranius, K. Börjesson, *Sci. Rep.* **2017**, *7*, 1–9.

[6] G. L. Burnett, H. T. Soh, J. Hawker, J. Read de Alaniz, *ChemComm* **2016**, *52*, 10525–10528.

[7] J. E. Yap, L. Zhang, J. T. Lovegrove, J. E. Beves, M. H. Stenzel, *Macromol. Rapid Commun.* **2020**, *2000236*, 1–8.

[8] M. M. Lerch, M. J. Hansen, W. A. Velema, W. Szymanski, B. L. Feringa, *Nat. Commun.* **2016**, *7*, 1–10.

[9] Y. J. Diaz, Z. A. Page, A. S. Knight, N. J. Treat, J. R. Hemmer, C. J. Hawker, J. Read de Alaniz, R. Hemmer, C. J. Hawker, J. Read de Alaniz, *Chem. - A Eur. J.* **2017**, *23*, 3562–3566.

[10] A. Balamurugan, H. Il Lee, *Macromolecules* **2016**, *49*, 2568–2574.

[11] S. Ulrich, S. O. Moura, Y. Diaz, M. Clerc, A. Géraldine, J. Read de Alaniz, A. Martins, N. M. Neves, M. Rottmar, R. M. Rossi, et al., *Sensors Actuators B. Chem.* **2020**, *322*, 128570.

[12] Q. Chen, Y. J. Diaz, M. C. Hawker, M. R. Martinez, Z. A. Page, S. X. Zhang, C. J. Hawker, J. Read de Alaniz, *Macromolecules* **2019**, *52*, 4370–4375.

[13] S. Seshadri, L. F. Gockowski, J. Lee, M. Sroda, M. E. Helgeson, J. Read de Alaniz, M. T. Valentine, *Nat. Commun.* **2020**, *11*, 1–8.

[14] N. Mallo, P. T. Brown, H. Iranmanesh, T. S. C. MacDonald, M. J. Teusner, J. B. Harper, G. E. Ball, J. E. Beves, *Chem. Commun.* **2016**, *52*, 13576–13579.

[15] M. M. Lerch, S. J. Wezenberg, W. Szymanski, B. L. Feringa, *J. Am. Chem. Soc.* **2016**, *138*, 6344–6347.

[16] M. M. Lerch, W. Szymański, B. L. Feringa, *Chem. Soc. Rev.* **2018**, *47*, 1910–1937.

[17] M. M. Lerch, M. Di Donato, A. D. Laurent, M. Medved', A. Iagatti, L. Bussotti, A. Lapini, W. J. Buma, P. Foggi, W. Szymański, et al., *Angew. Chemie - Int. Ed.* **2018**, *57*, 8063–8068.

[18] D. M. Sanchez, U. Raucci, K. N. Ferreras, T. J. Martínez, *J. Phys. Chem. Lett.* **2020**, *11*, 7901–7907.

[19] C. García-Iriepa, M. Marazzi, D. Sampedro, *ChemPhotoChem* **2019**, *3*, 866–873.

[20] N. Mallo, E. D. Foley, H. Iranmanesh, A. D. W. Kennedy, E. T. Luis, J. Ho, J. B. Harper, J. E. Beves, *Chem. Sci.* **2018**, *9*, 8242–8252.

[21] B. F. Lui, N. T. Tierce, F. Tong, M. M. Sroda, H. Lu, J. Read de Alaniz, C. J. Bardeen, *Photochem. Photobiol. Sci.* **2019**, *18*, 1587–1595.

[22] A. D. Laurent, M. Medved, D. Jacquemin, *ChemPhysChem* **2016**, *17*, 1846–1851.

[23] M. M. Lerch, M. Medved, A. Lapini, A. D. Laurent, A. Iagatti, L. Bussotti, W. Szymański, W. J. Buma, P. Foggi, M. Di Donato, et al., *J. Phys. Chem. A* **2018**, *122*, 955–964.

[24] L. Payne, J. D. Josephson, R. S. Murphy, B. D. Wagner, *Molecules* **2020**, *25*, 4928.

[25] D. G. Patel, M. M. Paquette, R. A. Kopelman, W. Kaminsky, M. J. Ferguson, N. L. Frank, *J. Am. Chem. Soc.* **2010**, *132*, 12568–12586.

[26] C. Reichardt, *Chem. Rev.* **1994**, *94*, 2319–2358.

[27] H. Zulfikri, M. A. J. Koenis, M. M. Lerch, M. Di, W. Szyma, C. Filippi, B. L. Feringa, W. J. Buma, *J. Am. Chem. Soc.* **2019**, *141*, 7376–7384.

[28] G. Sinawang, B. Wu, J. Wang, S. Li, Y. He, *Macromol. Chem. Phys.* **2016**, *217*, 2409–2414.

[29] S. Ulrich, J. R. Hemmer, Z. A. Page, N. D. Dolinski, O. Rifaie-graham, N. Bruns, C. J. Hawker, L. F. Boesel, J. Read de Alaniz, *ACS Macro Lett.* **2017**, *6*, 738–742.

[30] E. Yap, N. Mallo, M. H. Stenzel, D. S. Thomas, J. E. Beves, *Polym. Chem.* **2019**, *10*, 6515–6522.

[31] Y. Zhao, D. G. Truhlar, *Theor. Chem. Acc.* **2008**, *120*, 215–241.

[32] Y. Zhao, D. G. Truhlar, *Acc. Chem. Res.* **2008**, *41*, 157–167.

[33] A. V. Marenich, C. J. Cramer, D. G. Truhlar, *J. Phys. Chem. B* **2009**, *113*, 6378–6396.

[34] M. J. Frisch, G. W. Trucks, H. B. Schlegel, G. E. Scuseria, M. a. Robb, J. R. Cheeseman, G. Scalmani, V. Barone, G. a. Petersson, H. Nakatsuji, et al., **2016**, Gaussian 16, Revision C.01, Gaussian, Inc., Wallin.

Author Manuscript

This article is protected by copyright. All rights reserved

Entry for the Table of Contents

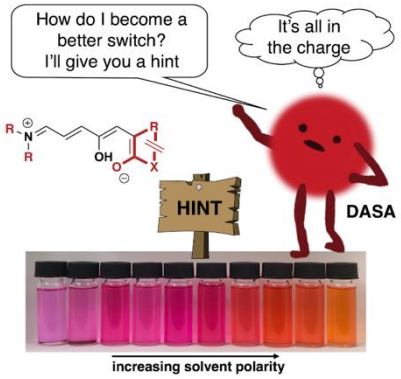

The effects of solution-state dielectric and intermolecular interactions on the degree of charge separation provides a route to understand the switching properties and concentration dependence of donor–acceptor Stenhouse adducts (DASAs). Using solvatochromic analysis of the open form DASA in conjunction with X-ray diffraction (XRD) and computational theory we analyzed the ionic character of a series of DASAs.

Institute and/or researcher Twitter usernames: @javier_read and @ReadAlanizteam

WILEY-VCH

Author Manuscript

This article is protected by copyright. All rights reserved